

Shewanella oneidensis as a living electrode for controlled radical polymerization

Gang Fan^{a,b,1}, Christopher M. Dundas^{a,1}, Austin J. Graham^a, Nathaniel A. Lynd^{a,b}, and Benjamin K. Keitz^{a,2}

^aMcKetta Department of Chemical Engineering, University of Texas at Austin, Austin, TX 78712; and ^bCenter for Dynamics and Control of Materials, University of Texas at Austin, Austin, TX 78712

Edited by Jeffrey A. Gralnick, University of Minnesota, St. Paul, MN, and accepted by Editorial Board Member Catherine J. Murphy March 19, 2018 (received for review January 16, 2018)

Metabolic engineering has facilitated the production of pharmaceuticals, fuels, and soft materials but is generally limited to optimizing well-defined metabolic pathways. We hypothesized that the reaction space available to metabolic engineering could be expanded by coupling extracellular electron transfer to the performance of an exogenous redox-active metal catalyst. Here we demonstrate that the electroactive bacterium Shewanella oneidensis can control the activity of a copper catalyst in atomtransfer radical polymerization (ATRP) via extracellular electron transfer. Using S. oneidensis, we achieved precise control over the molecular weight and polydispersity of a bioorthogonal polymer while similar organisms, such as Escherichia coli, showed no significant activity. We found that catalyst performance was a strong function of bacterial metabolism and specific electron transport proteins, both of which offer potential biological targets for future applications. Overall, our results suggest that manipulating extracellular electron transport pathways may be a general strategy for incorporating organometallic catalysis into the repertoire of metabolically controlled transformations.

metabolic engineering | polymerization | extracellular electron transport

etabolic engineering has provided alternative production pathways for the synthesis of pharmaceuticals (1), fuels (2), and soft materials by redirecting carbon flux toward specific metabolites (3). Despite significant progress, the reaction space available for metabolic engineering is still relatively limited compared with synthetic chemistry (4). One way to expand the scope of metabolic transformations is to leverage respiratory electron flux, which can be used for power generation, as in microbial fuel cells (5, 6), or inverted to produce metabolites from exogenously supplied electrons, as in bioelectrosynthesis (7, 8). The flexibility of these applications can be further extended by coupling metabolic transformations to processes that occur independently of the cell, such as nanoparticle photoexcitation or electrocatalytic hydrogen generation (9, 10). However, these advances are still generally limited to native metabolic intermediates and products.

In an effort to expand the power of microbial catalysis, we hypothesized that electron flux from metabolic activity could be adapted to control exogenous, bioorthogonal reactions via extracellular electron transfer to a redox-active metal catalyst. To test our hypothesis, we leveraged the electroactive bacterium Shewanella oneidensis MR-1. Similar to other electroactive bacteria (11, 12), MR-1 is able to transport electron equivalents over micrometer distances and has specialized machinery for moving electrons in and out of the cell (13, 14). Under anaerobic conditions, MR-1 consumes lactate, or other small carbon sources, and deposits electrons into redox-active organics, metals, and materials. Given the relatively negative potential of its terminal outer membrane cytochromes [~-350 to +50 mV vs. standard hydrogen electrode (SHE)] (15, 16), MR-1 is able to reduce a variety of soluble metals including U(VI), Cr(VI), Fe(III), V(V), and Mn(IV), as well as oxides such as hematite, ferrihydrite, and graphene oxide (17, 18). MR-1 can also respire onto electrodes poised at an appropriate potential (19). Overall, the unique

electron transport machinery and genetic tractability of MR-1 has made it a popular organism for use in microbial fuel cells (5, 6), bioelectrosynthesis (7, 8), and bioremediation (20, 21).

To explore if extracellular electron transfer from MR-1 could control the performance of an exogenous metal catalyst, we examined atom-transfer radical polymerization (ATRP). In ATRP, a redox-active metal catalyst reacts with a halogenated initiator to generate a radical that propagates through the addition of monomers or reacts with the newly oxidized catalyst to produce a dormant polymer chain (Fig. 1A) (22). The concentration of active radicals and polymerization rate is controlled by the redox equilibrium of the metal catalyst, which can be influenced through the application of an external potential (23–26). This suggests that an electroactive bacterium with appropriate redox capabilities, such as MR-1, could control catalysis in a similar manner to an electrode via direct extracellular electron transfer to the metal catalyst (27). Here we show that MR-1 can activate copper (Cu) catalysts for ATRP and that this mechanism is coupled to bacterial metabolism via specific electron transport proteins. Organisms lacking analogous extracellular electron transport machinery, such as *Escherichia coli*, showed minimal polymerization activity under our conditions. Polymerizations in the presence of MR-1 exhibited rates comparable to other aqueous controlled radical polymerizations and provided

Significance

Metabolic engineering benefits from the tunable and tightly controlled transformations afforded by biological systems. However, these reactions have generally been limited to naturally occurring pathways and products. In this work, we coopt metabolic electron transfer from *Shewanella oneidensis* to control the activity of an exogenous metal catalyst in an abiotic reaction scheme: atomtransfer radical polymerization. In the presence of *S. oneidensis*, polymerizations exhibited well-defined kinetics and yielded polymers with controlled molecular weights and low polydispersities. Additionally, polymerization activity was dependent on electroactive metabolism and specific electron transport proteins, both of which provide handles to control material synthesis. This work serves as a proof-of-principle toward expanding the scope of reactions available to metabolic engineers to include previously discovered transition-metal-catalyzed reactions.

Author contributions: G.F., C.M.D., A.J.G., N.A.L., and B.K.K. designed research; G.F., C.M.D., and A.J.G. performed research; N.A.L. contributed new reagents/analytic tools; G.F., C.M.D., A.J.G., and B.K.K. analyzed data; and G.F., C.M.D., A.J.G., and B.K.K. wrote the paper.

Conflict of interest statement: The authors have filed a patent based on this work.

This article is a PNAS Direct Submission. J.A.G. is a guest editor invited by the Editorial Board.

Published under the PNAS license.

Data deposition: Experimental data are publicly available through the Texas Data Repository (dx.doi.org/10.18738/T8/Q02FQU).

¹G.F. and C.M.D. contributed equally to this work.

²To whom correspondence should be addressed. Email: keitz@utexas.edu.

This article contains supporting information online at www.pnas.org/lookup/suppl/doi:10. 1073/pnas.1800869115/-/DCSupplemental.

Published online April 16, 2018.

Downloaded from https://www.pnas.org by 68.238.20.100 on November 28, 2023 from IP address 68.238.20.100.

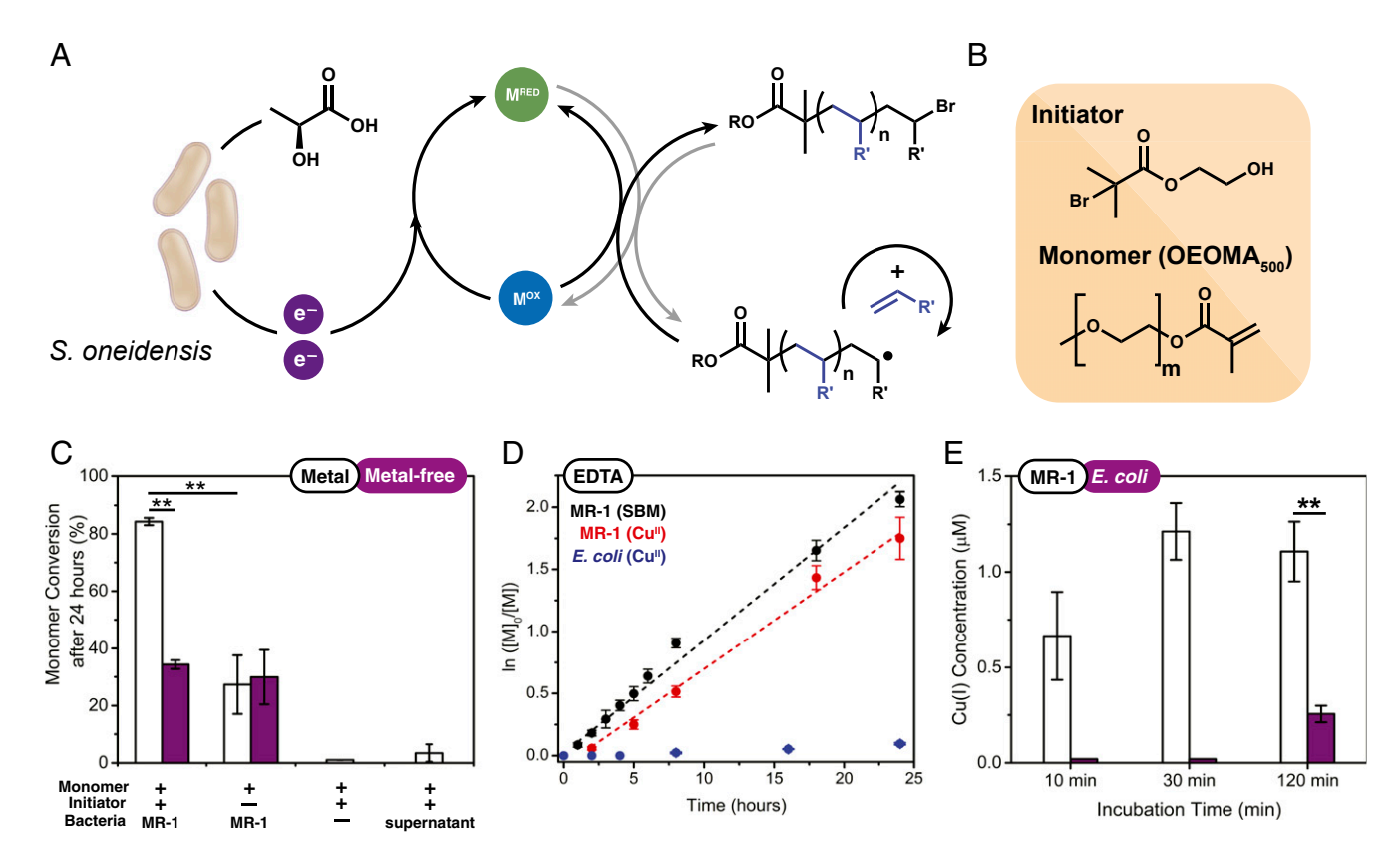


Fig. 1. S. oneidensis enabled ATRP and initial polymerization kinetics. (A) Electron equivalents generated from S. oneidensis MR-1 reduce a metal catalyst from an inactive state (M^{OX}) to an active state (M^{RED}). The active catalyst reacts with a halogenated initiator or polymer chain to produce a radical (gray arrow) that can polymerize olefins. The radical can also react with the now-deactivated catalyst (M^{OX}) to form a dormant chain (black arrow, Right). (B) ATRP initiator (HEBIB) and macromonomer (OEOMA₅₀₀) used in this study. (C) Monomer conversion after 24 h under various conditions with (white) and without (purple) trace metal mix added to bacterial media. (D) Kinetics of monomer conversion in MR-1 or E. coli culture using Cu(II)-EDTA as catalyst (E) Extracellular Cu(II) reduction monitored with the Cu(I) specific fluorescent dye CF4. Data show mean \pm SD of three independent experiments. **P < 0.01.

narrowly dispersed polymers with controlled molecular weights. Ultimately, our results demonstrate that extracellular electron transport can control redox-based catalysis and suggest that targeting biological electron transport pathways may combine the genetic tunability of metabolic engineering with the mechanismdriven design of organometallic catalysis.

Results

Exogenous Metals and S. oneidensis Enable ATRP. An anaerobic reaction mixture containing poly(ethylene glycol) methyl ether methacrylate monomer with $M_n = 500$ g/mol (OEOMA₅₀₀) and a halogenated initiator was inoculated with stationary-phase MR-1 (anaerobically pregrown with lactate/fumarate) (Fig. 1B). After 24 h, the solution became viscous and almost complete conversion of monomer was measured using ¹H NMR spectroscopy. As expected, no polymerization activity was observed under aerobic conditions. Cell-free and MR-1 supernatant controls also showed minimal monomer conversion. Bacterial pregrowth and reaction mixture balance volume was comprised of Shewanella basal medium (SBM), which contains EDTA and several redoxactive metals that could be functioning as catalysts (SI Appendix, Table S1). Reaction mixtures omitting these metals displayed significantly attenuated polymerization activity (Fig. 1C). Similarly, removal of initiator decreased monomer conversion after 24 h of MR-1 culture, independently of metal presence. We measured background radical polymerization activity in all reactions containing metabolically active cells. Contributors to this background polymerization could include bacterially secreted flavins and outer membrane heme-containing proteins. Flavins can act as radical initiators while heme-containing proteins have previously been used as catalysts for ATRP (28, 29). However,

the significant decrease in monomer conversion when exogenous metals were removed from solution suggests that it is primarily extracellular metal ions that act as catalysts. Following the kinetics of the polymerization, we discovered that metals, initiator, and MR-1 were all required to give well-controlled first-order kinetics in OEOMA₅₀₀ conversion, which is indicative of a constant radical concentration (SI Appendix, Fig. S1). Foregoing any of these components resulted in decreased monomer conversion and non-first-order polymerization kinetics. Together, these results confirm that exogenous metals and MR-1 are required for the controlled polymerization kinetics that are characteristic of ATRP.

Identification of Cu as a Viable ATRP Catalyst. Next, we identified the specific metal responsible for polymerization activity. Based on previous studies of ATRP (22), we hypothesized that polymerization activity could be primarily attributed to Shewanellainduced reduction of Cu(II) to Cu(I). Indeed, almost complete rescue of polymerization activity was observed when all exogenous metals were removed from the reaction culture except for CuSO₄·5H₂O and EDTA (Fig. 1D). We also briefly explored the activity of other known polymerization catalysts present in SBM. For example, both Fe(III) and Co(III) can be reduced by MR-1 and can serve as catalysts for ATRP and cobalt-mediated radical polymerization, respectively (30). Co(III)-porphyrins can also catalyze the radical-based dehalogenation of C-Cl bonds in the presence of MR-1 (27). We found that both FeSO₄ and Co(NO₃)₂ yielded polymerization activity above metal-free controls (SI Appendix, Fig. S2), but continued with Cu(II/I) since it is the most well-understood and established catalyst for ATRP. Notably, substituting E. coli MG1655 for MR-1 under otherwise identical conditions completely abolished polymerization activity

with Cu(II/I) as the catalyst (Fig. 1D). Additionally, we did not observe any significant polymerization activity under several alternative *E. coli* culture conditions. Overall, these results show that Cu(II/I) is an active catalyst for MR-1–enabled ATRP and suggest that the unique electron transport machinery of MR-1 is critical for polymerization activity.

ATRP activity in our system is contingent upon the MR-1controlled reduction of Cu(II) to Cu(I). Thus, we measured the extracellular concentration of Cu(I) using the Cu(I)-specific fluorescent probe Copper Fluor-4 (CF4) (31). Cultures of MR-1 were incubated with CuSO₄·5H₂O and CF4, spun down, and the extracellular concentration of Cu(I) measured via plate reader. Immediate reduction of Cu(II) was observed in the presence of MR-1, whereas E. coli controls showed minimal reduction on the same time scale (Fig. 1E). In eukaryotic systems, incubation with exogenous copper results in a measurable increase in free cytoplasmic Cu(I) (32). In contrast, bacteria quickly detect and sequester free Cu(I) (33). The effective concentration of free Cu(I) in bacterial cytoplasm is estimated to be in the attomolar (10⁻¹⁸ M) range and is difficult to detect (34). Consistent with these reports, we measured no significant increase in cytoplasmic Ĉu(I) (via flow cytometry) following incubation of MR-1 with CuSO₄·5H₂O and CF4 (SI Appendix, Fig. S7). Together, these data confirm that MR-1 extracellularly reduces Cu(II) and explain the observed differences in polymerization activity between MR-1 and E. coli.

Use of Tris(2-pyridylmethyl)amine Ligand Accelerates Polymerization Rate and Improves Control of Polymer Properties. Having demonstrated robust monomer conversion, we measured the properties of polymers formed with MR-1, Cu(II), and EDTA. Polymerization kinetics were well-controlled under these conditions, but polymer molecular weights were higher than expected based on the monomer-to-initiator ratio. Similarly, we measured a nonlinear dependence of molecular weight on monomer conversion (SI Appendix, Fig. S9). Under aqueous conditions, Cu(I) is prone to decomposition in the absence of a suitable ligand, which can lead to kinetic anomalies and uncontrolled molecular weights (23). Thus, we predicted that changing the ligand would yield improved control over polymer microstructure. We replaced EDTA with Tris(2pyridylmethyl)amine (TPMA), a well-known ligand for aqueous ATRP, and observed an immediate increase in polymerization rate. Complete conversion of OEOMA₅₀₀ occurred in ~2 h while cellfree, supernatant, and E. coli experiments showed no significant conversion. A higher molecular weight macromonomer, OEOMA₉₀₀, showed similar polymerization kinetics in the presence of MR-1 and Cu(II/I)-TPMA (SI Appendix, Fig. S13). Under optimized conditions, we achieved precise control over poly(OEOMA₅₀₀) molecular weight and measured a linear relationship between polymer molecular weight and conversion, indicative of a living polymerization (Fig. 2B).

Repeated addition of OEOMA $_{500}$ to the microbial culture yielded first-order kinetics with rate constants consistent with the initial addition (Fig. 2C). Moreover, we prepared diblock copolymers via sequential addition of OEOMA $_{500}$ and N-isopropylacrylamide (NIPAM) to the MR-1 culture (SI Appendix, Figs. S14 and S15). Combined, these results demonstrate the living nature of the polymerization, highlight its synthetic utility, and definitively show that the reaction is metal-catalyzed. Our data are also consistent with previous reports on aqueous ATRP describing the significant influence of catalyst stability on polymer conversion and microstructure.

Viable Bacteria Enable ATRP, Not Secreted or Released Reducing Factors. Having established that MR-1 facilitates ATRP, we next examined the biological factors that contribute to polymerization activity. Specifically, we investigated whether promiscuous cellular reductants or metabolic activity of viable bacteria were responsible for Cu(II) reduction and subsequent catalysis. The cytoplasm and periplasm of bacteria are reducing environments, easily capable of reducing Cu(II). Under stress conditions, cell lysis can release intracellular reductants and influence the overall redox potential of a microbial culture. Both E. coli and MR-1 can secrete reducing factors, such as glutathione and flavins, into the extracellular space (35-38). Secretion or release of metal ions, like Fe(II), could also cause Cu(II) reduction. We hypothesize that these effects may explain polymerization activity that was previously observed with E. coli and Pseudomonas aeruginosa (24). Indeed, polymerizations using glutathione as reductant showed dose-dependent polymerization activity, but polymerization rates were at least an order of magnitude slower relative to reactions containing MR-1 (SI Appendix, Fig. S16). Lysed MR-1 and E. coli also showed significant polymerization activity, consistent with the release of intracellular reducing factors. However, heat-killed cells from both species, which are metabolically inactive but retain membrane structure, showed no detectable polymerization activity (SI Appendix, Fig. S17). Combined with the minimal activity of supernatant from active MR-1 cultures, these results demonstrate that secreted reducing factors are not a significant contributor to polymerization activity in our system.

To further rule out cell lysis and assess the influence of Cu(II/I) toxicity on polymerization activity, we evaluated MR-1 and $E.\ coli$ viability under optimized polymerization conditions. Cu(II/I) is a potent microbial toxin, particularly under anaerobic conditions. Similar to Fe(III/II), Cu(II/I) can participate in Fenton chemistry and contribute to oxidative stress (39). In addition, copper can readily replace iron in enzyme cofactors, such as those in fumarate reductase (40). We speculated that Cu(II) supplementation may induce cell lysis, thereby contributing to polymerization activity. However, under aerobic conditions, we observed minimal inhibition of MR-1 growth when it was incubated with exogenous Cu(II) (5 μ M) ($SI\ Appendix$, Fig. S18). Switching to our standard reaction conditions, we measured no

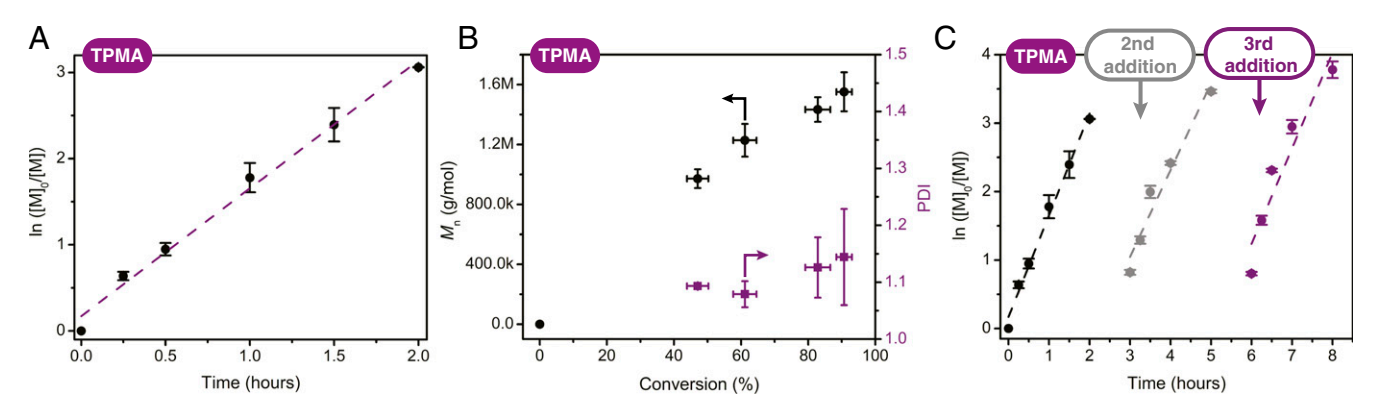


Fig. 2. Kinetics and properties of polymers formed with MR-1. (A) First-order kinetics for conversion of monomer over time using Cu(II)-TPMA with MR-1. (B) Molecular weight and polydispersity of poly(OEOMA₅₀₀) as a function of monomer conversion. (C) Repeated addition of OEOMA₅₀₀ monomer showing first-order kinetics and living nature of polymerization. Data show mean \pm SD of three independent experiments.

Downloaded from https://www.pnas.org by 68.238.20.100 on November 28, 2023 from IP address 68.238.20.100.

significant difference in MR-1 colony-forming units (CFUs) following polymerization (SI Appendix, Fig. S19). Similarly, bacterial viability measurements, assessed via fluorescence microscopy, showed minimal loss in cell viability for both MR-1 (74% viable) and E. coli (86% viable) under typical polymerization conditions and corroborated our CFU counts (SI Appendix, Fig. S20). Moreover, scanning electron micrographs revealed that polymer was extracellular and closely associated with intact MR-1 (SI Appendix, Fig. S22). Finally, we note that the Cu(II/I) concentrations (2 µM and below) used in our studies are significantly lower than levels reported to induce a microbial stress response in MR-1 (41). Together, these data suggest that the Cu(II/I) concentrations and monomer/initiator used for our polymerizations do not elicit a stress response that can explain polymerization activity.

Carbon Source Affects Polymerization Kinetics. To investigate the extent of metabolic control over catalyst performance, we examined the effect of carbon source on polymerization activity. Carbon source affects electron flux through the central metabolism of MR-1 and should influence polymerization rate if they are coupled (Fig. 3A). With TPMA as the ligand, we found that MR-1 fed with lactate, which generates four electron equivalents per molecule, yielded the fastest rate of polymerization (Fig. 3B). In contrast, starved cells showed lower polymerization activity, as did cells fed with acetate, which cannot be used as a carbon source by MR-1 under anaerobic conditions (42). MR-1 supplied with pyruvate, which yields two electron equivalents per molecule, showed polymerization activity between lactate- and acetate-fed/starved cells. The residual activity observed in starved and acetate-fed cells is likely due to latent metabolic activity from growth in rich media or from residual electron density on the outer membrane cytochromes, both of which have been observed for MR-1 and Geobacter sulfurreducens (18, 43). The short time scale (<2 h) of reactions conducted using TPMA also makes it challenging to observe metabolic effects. Replacing TPMA with EDTA resulted in a larger difference between lactate-fed and starved cells, likely because the longer time scale of these polymerizations (24 h) accentuated metabolic differences (SI Appendix, Fig. S23). The EDTA experiments also suggest that continuous metabolic activity and associated Cu(II) reduction counters catalyst deactivation when a less supportive ligand is used (23). In sum, these results demonstrate that polymerization rate is strongly coupled to metabolic activity and subsequent electron flux.

MtrC Expression Is Critical for ATRP Activity. MR-1 uses specialized respiratory pathways to transport electron equivalents from the cytoplasm and periplasm to the extracellular space (Fig. 4A) (13, 44). To understand how the components of these pathways influence ATRP activity, we measured the effect of knocking out select cytochromes and other redox-relevant proteins on polymerization kinetics. Molecular hydrogen and flavins are strong reductants generated by MR-1 that may participate in Cu(II) reduction (45, 46). However, knockouts of periplasmic hydrogenases $(\Delta hydA\Delta hyaB)$ and an inner-membrane flavin exporter (Δbfe) exhibited no difference in monomer conversion compared with MR-1. In contrast, a mutant lacking outer-membrane cytochromes $(\Delta mtrC\Delta omcA)$ showed significantly attenuated polymerization rates (Fig. 4B). MtrC is a key decaheme c-type cytochrome through which MR-1 interacts with metals and metal oxides; our results suggest that it is also important for Cu(II) reduction (14). E. coli cytochromes are not homologous to MtrC and the organism largely lacks the cytochrome content of MR-1 (42 cytochrome genes in MR-1 vs. 5-7 in E. coli) (47). This deficiency in extracellular electron transport machinery explains why E. coli showed minimal polymerization activity. Complete abolishment of activity was not observed for the $\Delta mtrC\Delta omcA$ mutant because it is unlikely that Cu(II) reduction is completely tied to an exclusive cytochrome reduction pathway. MR-1 expresses several other electron transfer proteins that could mediate Cu(II) reduction and their transcription levels appear agnostic toward different soluble

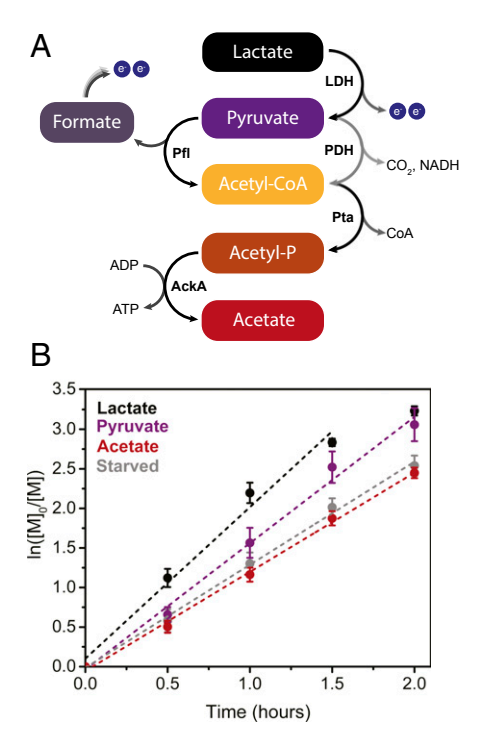


Fig. 3. Polymerization activity is controlled by electroactive metabolism. (A) Simplified carbon metabolism of S. oneidensis. (B) Polymerization kinetics for MR-1 supplied with different carbon sources using Cu(II)-TPMA as catalyst. Data show mean \pm SD of three independent experiments. Statistical analysis for B is presented in SI Appendix, Fig. S24.

electron acceptors (17). MR-1 also possesses outer-membrane cytochromes other than MtrC (e.g., MtrF), which can compensate for its absence (48). We attempted to inhibit all outermembrane cytochromes using KCN, but found that this also disrupted positive polymerization controls. Notably, normal polymerization activity was partially rescued after complementation with a plasmid encoding MtrC (Fig. 4C). This finding is consistent with previous reports showing that MtrC alone is sufficient to rescue the majority of electron transfer activity and that OmcA is not required for the Mtr pathway to function (48). More importantly, the complementation result suggests that polymerization activity can be controlled by manipulating MtrC expression. Altogether, our results highlight the unique role that outer-membrane cytochromes play in extracellular electron transport and offer additional support for a specific and manipulable link between metabolic activity and catalyst performance.

Discussion

In this study, we evaluated the ability of an electroactive bacteria to control an extracellular metal-catalyzed reaction. The majority of reports describing nonenzymatic metal catalysis in the presence of cells have focused on developing new reactions for bioorthogonal labeling or prodrug activation (49, 50). These reactions are compatible with the cellular environment, but are generally not under metabolic control. In contrast, several metabolic engineering efforts have coupled abiotic catalytic cycles to cellular metabolism through the use of secondary metabolites such as hydrogen, formate, and other small molecules, or through bioelectrochemical cells (5, 7, 9, 51). Synthesizing aspects of these fields, we showed that respiratory electron flux can be directly harnessed to control the performance of a metal-catalyzed polymerization and that extracellular electron transfer proteins are a critical enabler of this process.

Radical polymerizations in the presence of MR-1 and Cu(II/I)-TPMA were very well-controlled. We initially chose OEOMA₅₀₀ as a monomer because it is common in aqueous radical polymerizations and allows for quantitative rate comparisons between polymerization

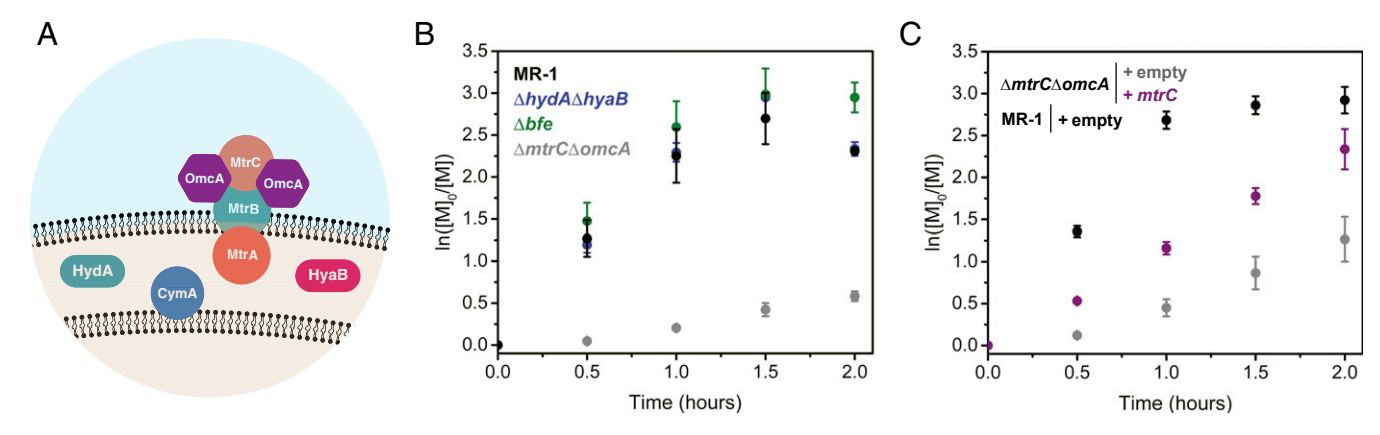


Fig. 4. Electron transfer proteins impact polymerization kinetics. (A) Key proteins involved in extracellular electron transport in MR-1. (B) Effect of gene knockouts on polymerization activity using Cu(II)-TPMA. (C) Rescue of normal polymerization activity via complementation with a plasmid encoding MtrC, using Cu(II)-TPMA as a catalyst. Data show mean \pm SD of three independent experiments. Statistical analysis for B and C is presented in SI Appendix, Figs. S25 and S26, respectively.

methodologies. Under optimized conditions, the rate of polymerization was first order with a rate constant comparable to polymerizations conducted in the presence of an external electrode (52). Specifically, MR-1 with Cu(II/I)-TPMA polymerized OEOMA₅₀₀ with a rate constant of 2.20 h⁻¹ at 30 °C while electrochemical ATRP under similar conditions yielded a rate constant of $\sim 1.52 \text{ h}^{-1}$ at 25 °C (52). We measured similar rate constants under several alternative conditions (SI Appendix, Table S5). Also similar to electrochemical ATRP, we found that very low concentrations of catalyst $(0.2 \mu M)$ were sufficient for polymerization activity. In contrast, polymerizations conducted in the presence of a sacrificial reductant require higher catalyst concentrations (22). Polymerizations in the presence of MR-1 yielded polymers with well-defined molecular weights and narrow molecular weight distributions. We also highlighted the synthetic utility of our polymerization by preparing diblock copolymers with controlled molecular weight using OEOMA₅₀₀ and NIPAM as monomers. Similar polymers have been used for self-assembly, drug delivery, and other applications (53). Alternatively, polymers with well-defined microstructure could be used to coat bacterial cells, providing protection from toxins or initiating biofilm phenotypes (54, 55). Given our results, it is likely that a wide variety of applications relying on water-soluble polymers can leverage S. oneidensis controlled polymerization.

By probing the biology of S. oneidensis controlled ATRP, we demonstrated that electroactive metabolism and polymerization activity are highly coupled. The catabolic pathways controlling electron flux exerted significant influence on polymerization rate, which makes them promising targets for future engineering applications. For example, pathways for utilization of different carbon sources (e.g., glucose, glycerol, xylose) or increasing electron-equivalent flux to the inner membrane via NADH dehydrogenase overexpression could be integrated into S. oneidensis to modulate Cu(II) reduction (56-58). Alternatively, controlling the expression of electron transfer proteins could be used to tune polymerization activity. Toward this goal, we identified MtrC as an important regulator of polymerization activity in S. oneidensis. Although E. coli does not natively possess cytochromes that are homologous to MtrC, the Mtr pathway can be heterologously expressed in it (59); this offers a potential means to adapt our polymerization system into a standard chassis organism. Other electroactive bacteria with outer-membrane cytochromes, such as G. sulfurreducens, could also be used to control polymerization activity (60). Overall, we found that MtrC serves as a master controller of polymerization activity and believe that it is a promising biological target for future optimization and synthetic biology applications involving extracellular metal catalysis.

In conclusion, we discovered that *S. oneidensis* MR-1 can effectively control polymerization activity in the absence of an electrode via extracellular electron transfer to a redox-active metal

catalyst. Polymers formed in the presence of S. oneidensis and Cu(II/I) were narrowly dispersed with defined molecular weights indicative of a living polymerization. Furthermore, polymerization kinetics were strongly dependent on catalyst structure, metabolic activity, and specific electron transport proteins. Future work may focus on optimizing both the chemical (e.g., ligand design) and biological (e.g., cytochrome expression) components of our system. More importantly, the reduction potential of MR-1 combined with the wealth of chemical transformations enabled by redox-active transition metals suggests that our system can be readily expanded to reactions beyond polymerization. Overall, our results demonstrate that the metabolic activity of an electroactive bacterium can be coupled to the performance of a redox-active metal catalyst and indicate that engineering of bacterial electron transport pathways may provide a general template for adapting traditional metalcatalyzed reactions for use in metabolic engineering.

Materials and Methods

All stock solutions and reaction mixtures were prepared in an anaerobic glove box. Before polymerizations, stock solutions of HEBIB (100× stock, 2.9 μ L in 287 μ L SBM containing casamino acids) and Cu-EDTA (200x stock from 10 mg CuSO₄·5H₂O in 1 L of 1.35 mM EDTA buffer) or Cu-TPMA (200× stock from 8.9 mg CuBr₂ and 11.6 mg TPMA in 100 mL DMF) were mixed. Afterward, a 2 mL polymerization reaction mixture was prepared as follows. To a sterile polypropylene culture tube was added 60% wt/wt sodium lactate solution (5.7 μL), 1 M fumarate solution (80 μ L), OEOMA₅₀₀ (92.6 μ L, 200 μ mol), HEBIB (2.9 μ L of 100× stock), Cu-EDTA (10 μ L of a 200× aqueous stock) or Cu-TMPA (10 μ L of a 200× DMF stock), and a balance of SBM lacking trace mineral mix. Final concentrations were lactate (20 mM), fumarate (40 mM), OEOMA₅₀₀ (0.1 M), HEBIB (0.1 mM), and Cu-EDTA (0.2 μ M) or Cu-TPMA (2.0 μ M). For reactions with different carbon sources, lactate was replaced with sodium pyruvate (20 mM) or sodium acetate (20 mM). Polymerization was initiated by adding 20 μL of 100× cell stock ($OD_{600} = 2.0$) to bring the final reaction volume to 2 mL and starting bacterial OD₆₀₀ to 0.02. Final reaction mixtures were incubated at 30 °C (S. oneidensis) or 37 °C (E. coli). Time points were aliquoted, diluted with deuterium oxide or GPC solvents, exposed to air to guench the reaction, then flash frozen in liquid N₂. Aliquots were stored at -20 °C until analysis via NMR spectroscopy or GPC.

ACKNOWLEDGMENTS. We thank Gauri Bora and Riley Shuping for their experimental assistance. *S. oneidensis* knockouts Δbfe , $\Delta hydA\Delta hyaB$, and $\Delta mtrC\Delta omcA$ were a generous gift from Prof. Jeffrey Gralnick. *E. coli* strain MG1655 was a generous gift from Prof. Lydia Contreras. Fluorescent dyes for Cu(I) detection (CF4, CTRL-CF4) were generously provided by Prof. Chris Chang. We gratefully acknowledge the use of facilities within the core microscopy lab of the Institute for Cellular and Molecular Biology, University of Texas at Austin. This research was supported by the Welch Foundation (Grants F-1929 and F-1904) and partially supported by the National Science Foundation through the Center for Dynamics and Control of Materials: an NSF Materials Research Science and Engineering Center under Cooperative Agreement DMR-1720595. NMR spectra were collected on a Bruker Avance III 500 funded by the NIH (Award 1 S10 OD021508-01).

Downloaded from https://www.pnas.org by 68.238.20.100 on November 28, 2023 from IP address 68.238.20.100.

- 1. Ro D-K, et al. (2006) Production of the antimalarial drug precursor artemisinic acid in engineered yeast. Nature 440:940-943.
- Blazeck J, et al. (2014) Harnessing Yarrowia lipolytica lipogenesis to create a platform for lipid and biofuel production. Nat Commun 5:3131.
- 3. Florea M, et al. (2016) Engineering control of bacterial cellulose production using a genetic toolkit and a new cellulose-producing strain. Proc Natl Acad Sci USA 113:E3431–E3440.
- 4. Keasling JD (2010) Manufacturing molecules through metabolic engineering. Science 330:1355-1358
- 5. Malvankar NS, Lovley DR (2014) Microbial nanowires for bioenergy applications. Curr Opin Biotechnol 27:88-95.
- 6. Yang Y, et al. (2015) Enhancing bidirectional electron transfer of Shewanella oneidensis by a synthetic flavin pathway. ACS Synth Biol 4:815–823.
- Rabaey K, Rozendal RA (2010) Microbial electrosynthesis-Revisiting the electrical route for microbial production. Nat Rev Microbiol 8:706-716.
- Ross DE, Flynn JM, Baron DB, Gralnick JA, Bond DR (2011) Towards electrosynthesis in shewanella: Energetics of reversing the mtr pathway for reductive metabolism. PLoS
- 9. Nichols EM, et al. (2015) Hybrid bioinorganic approach to solar-to-chemical conversion. Proc Natl Acad Sci USA 112:11461-11466.
- 10. Sakimoto KK, Wong AB, Yang P (2016) Self-photosensitization of nonphotosynthetic bacteria for solar-to-chemical production. Science 351:74-77.
- 11. Sydow A, Krieg T, Mayer F, Schrader J, Holtmann D (2014) Electroactive bacteria-Molecular mechanisms and genetic tools. Appl Microbiol Biotechnol 98:8481–8495.
- 12. Shi L, et al. (2016) Extracellular electron transfer mechanisms between microorganisms and minerals. Nat Rev Microbiol 14:651-662.
- 13. Pirbadian S. et al. (2014) Shewanella oneidensis MR-1 nanowires are outer membrane and periplasmic extensions of the extracellular electron transport components. Proc Natl Acad Sci USA 111:12883-12888.
- White GF, et al. (2013) Rapid electron exchange between surface-exposed bacterial cytochromes and Fe(III) minerals. Proc Natl Acad Sci USA 110:6346-6351.
- Schuergers N, Werlang C, Ajo-Franklin CM, Boghossian AA (2017) A synthetic biology approach to engineering living photovoltaics. Energy Environ Sci 10:1102–1115.
- Zacharoff LA, El-Naggar MY (2017) Redox conduction in biofilms: From respiration to living electronics. Curr Opin Electrochem 4:182-189.
- Beliaev AS, et al. (2005) Global transcriptome analysis of Shewanella oneidensis MR-1 exposed to different terminal electron acceptors. J Bacteriol 187:7138-7145
- 18. Flynn TM, O'Loughlin EJ, Mishra B, DiChristina TJ, Kemner KM (2014) Sulfur-mediated electron shuttling during bacterial iron reduction. Science 344:1039–1042.
- 19. Kim HJ, et al. (2002) A mediator-less microbial fuel cell using a metal reducing bacterium, Shewanella putrefaciens. Enzyme Microb Technol 30:145-152.
- 20. Sekar R, DiChristina TJ (2014) Microbially driven Fenton reaction for degradation of the widespread environmental contaminant 1,4-dioxane. Environ Sci Technol 48:12858–12867.
- 21. Marshall MJ, et al. (2006) c-type cytochrome-dependent formation of U(IV) nanoparticles by Shewanella oneidensis. PLoS Biol 4:e268.
- 22. Boyer C, et al. (2016) Copper-mediated living radical polymerization (atom transfer radical polymerization and copper(0) mediated polymerization): From fundamentals to bioapplications. Chem Rev 116:1803-1949.
- 23. Simakova A, Averick SE, Konkolewicz D, Matyjaszewski K (2012) Aqueous ARGET ATRP. Macromolecules 45:6371-6379.
- Magennis EP, et al. (2014) Bacteria-instructed synthesis of polymers for self-selective microbial binding and labelling. Nat Mater 13:748-755.
- 25. Niu J, et al. (2017) Engineering live cell surfaces with functional polymers via cytocompatible controlled radical polymerization. Nat Chem 9:537–545
- Magenau AJD, Strandwitz NC, Gennaro A, Matyjaszewski K (2011) Electrochemically mediated atom transfer radical polymerization. Science 332:81-84
- 27. Workman DJ, Woods SL, Gorby YA, Fredrickson JK, Truex MJ (1997) Microbial reduction of vitamin B12 by shewanella alga Strain BrY with subsequent transformation of carbon tetrachloride. Environ Sci Technol 31:2292-2297.
- Encinas MV, Rufs AM, Bertolotti S, Previtali CM (2001) Free radical polymerization photoinitiated by riboflavin/amines. Effect of the amine structure. Macromolecules 34:2845-2847.
- Simakova A, Mackenzie M, Averick SE, Park S, Matyjaszewski K (2013) Bioinspired iron-based catalyst for atom transfer radical polymerization. Angew Chem Int Ed Engl 52:12148-12151.
- 30. Peng C-H, Yang T-Y, Zhao Y, Fu X (2014) Reversible deactivation radical polymerization mediated by cobalt complexes: Recent progress and perspectives. Org Biomol Chem 12:8580-8587
- 31. Heffern MC, et al. (2016) In vivo bioluminescence imaging reveals copper deficiency in a murine model of nonalcoholic fatty liver disease. Proc Natl Acad Sci USA 113:14219-14224.

- 32. Cotruvo JA, Jr, Aron AT, Ramos-Torres KM, Chang CJ (2015) Synthetic fluorescent probes for studying copper in biological systems. Chem Soc Rev 44:4400–4414.
- 33. Changela A, et al. (2003) Molecular basis of metal-ion selectivity and zeptomola sensitivity by CueR. Science 301:1383-1387.
- 34. Chandrangsu P, Rensing C, Helmann JD (2017) Metal homeostasis and resistance in bacteria. Nat Rev Microbiol 15:338-350.
- 35. Smirnova GV, Oktyabrsky ON (2005) Glutathione in bacteria. Biochemistry (Mosc) 70: 1199-1211.
- 36. Helbig K, Bleuel C, Krauss GJ, Nies DH (2008) Glutathione and transition-metal homeostasis in Escherichia coli. J Bacteriol 190:5431-5438
- 37. Sporer AJ. Kahl LJ. Price-Whelan A. Dietrich LEP (2017) Redox-based regulation of bacterial development and behavior. Annu Rev Biochem 86:777-797.
- 38. Marsili E. et al. (2008) Shewanella secretes flavins that mediate extracellular electron transfer. Proc Natl Acad Sci USA 105:3968-3973.
- 39. Braymer JJ, Giedroc DP (2014) Recent developments in copper and zinc homeostasis in bacterial pathogens. Curr Opin Chem Biol 19:59-66.
- 40. Fung DKC, Lau WY, Chan WT, Yan A (2013) Copper efflux is induced during anaerobic amino acid limitation in Escherichia coli to protect iron-sulfur cluster enzymes and biogenesis. J Bacteriol 195:4556-4568.
- 41. Toes ACM, Daleke MH, Kuenen JG, Muyzer G (2008) Expression of copA and cusA in Shewanella during copper stress. Microbiology 154:2709-2718.
- 42. Pinchuk GE, et al. (2011) Pyruvate and lactate metabolism by Shewanella oneidensis MR-1 under fermentation, oxygen limitation, and fumarate respiration conditions. Appl Environ Microbiol 77:8234–8240
- 43. Esteve-Núñez A, Sosnik J, Visconti P, Lovley DR (2008) Fluorescent properties of c-type cytochromes reveal their potential role as an extracytoplasmic electron sink in Geobacter sulfurreducens. Environ Microbiol 10:497-505.
- 44. Breuer M, Rosso KM, Blumberger J (2014) Electron flow in multiheme bacterial cytochromes is a balancing act between heme electronic interaction and redox potentials. Proc Natl Acad Sci USA 111:611-616.
- 45. Glasser NR, Saunders SH, Newman DK (2017) The colorful world of extracellular electron shuttles. Annu Rev Microbiol 71:731-751.
- Meshulam-Simon G, Behrens S, Choo AD, Spormann AM (2007) Hydrogen metabolism in Shewanella oneidensis MR-1. Appl Environ Microbiol 73:1153-1165.
- 47. Meyer TE, et al. (2004) Identification of 42 possible cytochrome C genes in the Shewanella oneidensis genome and characterization of six soluble cytochromes. OMICS 8:57-77
- 48. Coursolle D. Gralnick JA (2010) Modularity of the Mtr respiratory pathway of Shewanella oneidensis strain MR-1. Mol Microbiol 77:995-1008.
- 49. Tonga GY, et al. (2015) Supramolecular regulation of bioorthogonal catalysis in cells using nanoparticle-embedded transition metal catalysts. Nat Chem 7:597-603.
- 50. Wang J, et al. (2016) Palladium-triggered chemical rescue of intracellular proteins via genetically encoded allene-caged tyrosine. J Am Chem Soc 138:15118-15121.
- 51. Sirasani G, Tong L, Balskus EP (2014) A biocompatible alkene hydrogenation merges organic synthesis with microbial metabolism. Angew Chem Int Ed Engl 53:7785-7788.
- 52. Bortolamei N, Isse AA, Magenau AJD, Gennaro A, Matyjaszewski K (2011) Controlled aqueous atom transfer radical polymerization with electrochemical generation of the active catalyst. Angew Chem Int Ed Engl 50:11391-11394.
- 53. Canning SL, Smith GN, Armes SP (2016) A critical appraisal of RAFT-mediated polymerization-induced self-assembly. Macromolecules 49:1985-2001
- 54. Park JH, Hong D, Lee J, Choi IS (2016) Cell-in-shell hybrids: Chemical nanoencapsulation of individual cells, Acc Chem Res 49:792-800.
- 55. Lui LT, et al. (2013) Bacteria clustering by polymers induces the expression of quorumsensing-controlled phenotypes. Nat Chem 5:1058-1065.
- 56. Choi D, et al. (2014) Metabolically engineered glucose-utilizing Shewanella strains under anaerobic conditions. Bioresour Technol 154:59-66.
- 57. Flynn JM, Ross DE, Hunt KA, Bond DR, Gralnick JA (2010) Enabling unbalanced fermentations by using engineered electrode-interfaced bacteria. MBio 1:e00190-10-e00190-17
- Tao L, et al. (2016) Improving electron trans-inner membrane movements in microbial electrocatalysts. Chem Commun (Camb) 52:6292-6295.
- 59. Jensen HM, TerAvest MA, Kokish MG, Ajo-Franklin CM (2016) CymA and exogenous flavins improve extracellular electron transfer and couple it to cell growth in Mtrexpressing Escherichia coli. ACS Synth Biol 5:679-688.
- 60. Kracke F. Vassilev I. Krömer JO (2015) Microbial electron transport and energy conservation-The foundation for optimizing bioelectrochemical systems. Front Microbiol 6:575.